RSC Advances

ROYAL SOCIETY OF CHEMISTRY

www.rsc.org/advances

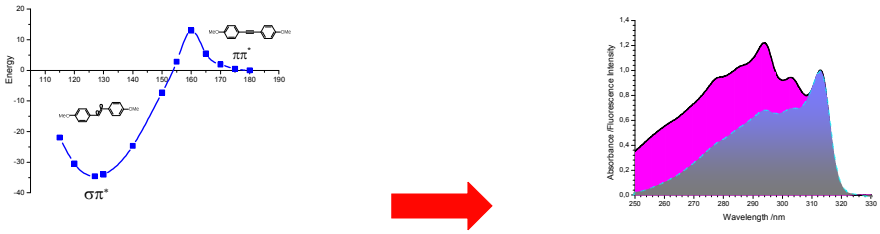

RCS Advances

RSCPublishing

ARTICLE

Experimental and theoretical studies of the spectroscopic properties of simple symmetrically substituted diphenylacetylene derivatives†

Małgorzata Wierzbicka, Irena Bylińska, Cezary Czaplewski, Wiesław Wiczk*

Cite this: DOI: 10.1039/xoxxoooooox

Received ooth January 2012,
Accepted ooth January 2012

DOI: 10.1039/xoxxoooooox

www.rsc.org/

The first two authors contributed equally to the work

A series of symmetrically substituted diphenylacetylene (DPA) derivatives possessing electron-donating (N,N-dimethylamino or methoxy) or electron-accepting (nitrile, ester or aldehyde) character were prepared and studied with respect to their spectral and photophysical properties. The photophysical characteristics of these compounds were studied in relation to their structures and influence of temperature. The observed spectral and photophysical properties are explained with the help of potential energy maps obtained from density functional theory (DFT, B3LYP, def2TZVP basis set) calculations. The structure-property relationships of all of the compounds are discussed.

1. Introduction

Conjugated organic polymers containing acetylene units have been the subject of intense research in the recent past[1-3]. In particular, they have been found to be substitutes for conventional materials in electronic or photonic devices[4], molecular wires[5], light emitting diodes[6-8], solar cells[9-12] and in electrogenerated chemiluminescence[13-18]. Asymmetric acetylene derivatives containing polycyclic aromatic or hetero-aromatic hydrocarbon substituent on one side and phenyl or its derivative on the second side show intense fluorescence[12-19]. Likewise, rather rigid, highly conjugated poly(p-phenylenethynylene)s are strongly fluorescing[20-30]. 1,2-diphenylethyne (tolane, DPA) and diphenylbuta-1,3-diyne behave quite differently. The photophysics of the two simplest aryl derivatives of acetylene and diacetylene were studied both experimentally[28,31-42] and theoretically[43-45]. These studies mainly concerned DPA, while diphenyldiacetylene was studied to a much lesser extent[39,42]. One of the most interesting photophysical properties of DPA is the loss of fluorescence that occurs following excitation of higher vibronic levels of the $1B_{1u}$ state under collision-free conditions of a supersonic free jet[31]. It also exhibits a strong temperature dependence of fluorescence quantum yield in solution[35]. The results of theoretical calculations made by Zgierski and Lim[43,45] indicate that while the lowest-energy excited singlet state is the B_{1u} ($\pi\pi^*$) state in the linear D_{2h} symmetry, the non-fluorescent $\pi\sigma^*$ state of A_u symmetry is the lowest in energy in the bent C_{2h} symmetry. This leads to the crossing of the fluorescent $\pi\pi^*$ and dark $\pi\sigma^*$ state potential energy curves. The transition from initial excited $\pi\pi^*$ state to $\pi\sigma^*$ state requires crossing a small energy barrier, which explains the loss of fluorescence in the gas phase at higher excitation energies and the thermally activated quenching of fluorescence in solution. The calculations also predict that the $\pi\sigma^*$ state of bent geometry can be identified by the reduced frequency of the acetylenic C≡C stretch because of the reduction in bond order and a strong $\pi\sigma^*\leftarrow\pi\sigma^*$ absorption at about 700 nm. The predictions arising from the calculations were confirmed experimentally. From picosecond time-resolved CARS spectroscopy[36,38], it was found that the central CC stretch frequency in the S_1 state is lower than 1600 cm^{-1} (1547 cm^{-1} predicted from theoretical calculations[43]) indicating a marked decrease of the C≡C bond order. Additionally, IR and CARS spectra suggested that the S_1 state of DPA has a planar trans-bent structure with a centre of symmetry[38]. The presence of an absorbance between $\pi\sigma^*\leftarrow\pi\sigma^*$ states at about 700 nm was confirmed experimentally[32,37,42]. The calculations made by Zgierski and Lim also predicted that the attachment of an electron-withdrawing group to DPA would increase the energy of the $\pi\sigma^*$ state and the $\pi\pi^*\leftarrow\pi\sigma^*$ state switch would not be expected to occur. Moreover, the attachment of an electron-donating group to DPA enhanced the state switch from an initially excited $\pi\pi^*$ to $\pi\sigma^*$ state. Also, these predictions have been experimentally confirmed by picosecond transient absorption spectroscopy. The transient absorption at about 700 nm for mono- and di-substituted DPA derivatives containing electron-donating groups, as well as a lack of such a transient absorption in this range of spectra for derivatives containing electron-withdrawing groups[37,43,45] have been registered.

DPA derivatives were mostly studied with an emphasis on theoretical calculations and picosecond absorption spectroscopy. Because there is not much information about fluorescence spectroscopy, here we present results of the photophysical studies of symmetrically substituted DPA derivatives. The studies include measurements of the absorption and emission spectra in solvents of different viscosities at room

and liquid nitrogen temperatures to investigate the effects of viscosity of the medium on the photophysical properties of the studied compounds. Moreover, the rotation energy barriers in the ground and excited state were calculated and compared to experimental literature data. The potential energy curves of the excited state for different bending angles were calculated using the DFT method. These data were used to determine the influence of the type of the substituent on the possibility of ππ* and πσ* state crossing.

The structure and atom numbering of compounds studied in this paper are presented in Fig. 1.

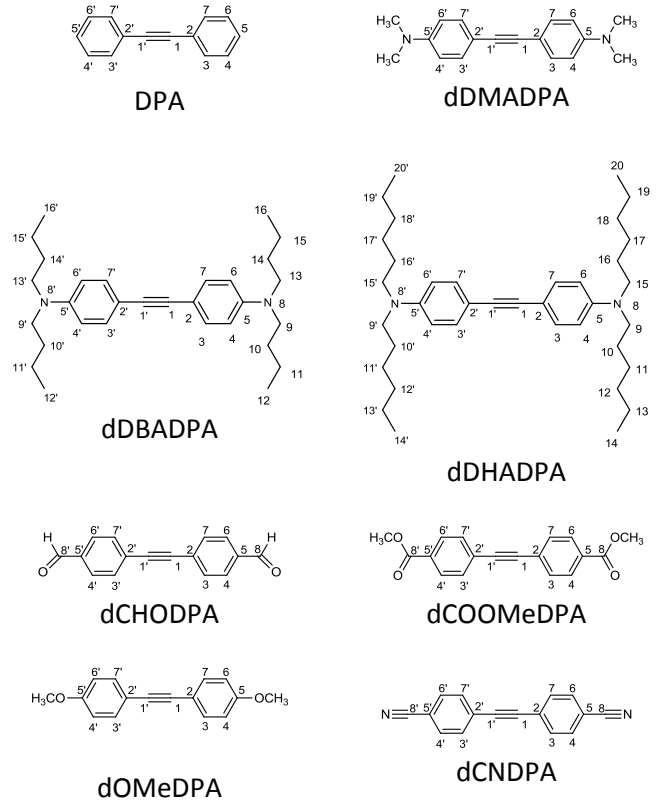

Fig 1. Structure and numbering of studied compounds.

2. Materials and methods

The progress of all reactions was monitored by TLC using Merck plates, Kieselgel 60 F254. The products were isolated by means of column chromatography (Merck, Kieselgel 60 (0.040-0.063 mm) and/or semi-preparative RP-HPLC (Kromasil column, C-8, 5 µm, 250 mm long, i.d. 20 mm).

The identification of the product was based on: ^{1}H and ^{13}C NMR spectra recorded on a Bruker AVANCE III (500 MHz) spectrometer in $CDCl_3$, mass spectra recorded on a Bruker Daltonics (HCTultra) instrument and Raman spectra recorded on a FRA-106 instrument (details are described in ESI).

2.1 Synthesis

Iodobenzene, 1-iodo-4-methoxybenzene, methyl-4-iodobenzoate, 4-iodobenzonitrile, 4-((trimethylsilyl)ethynyl)-benzaldehyde, phenylacetylene, 4-ethynylanisole, 4-ethynyl-N,N-dimethylaniline, ethynyltrimethylsilane, and bis(triphenyl-phosphine)palladium(II) dichloride (Sigma Aldrich), 4-bromo-benzaldehyde (Lancaster), 2-methyl-3-butyn-2-ol (Fluka) and N,N-dimethylaniline (P.P.H) were commercially available and used without further purification.

Synthesis of 4-iodo-N,N-dialkylaniline (1a-3a) (Scheme 1 ESI) were synthesized according to a procedure described in the literature[46].

A general scheme for the synthesis of acetylene derivatives is shown in Scheme 2 ESI. Protected acetylene derivatives (2b, 3b, 7b, 8b) and symmetrically substituted acetylene derivatives (4,4'-(ethyne-1,2-diyl)bis(N,N-dimethylaniline) (dDMADPA), 4,4'-(ethyne-1,2-diyl)bis(N,N-dibutylaniline) (dDBADPA), 4,4'-(ethyne-1,2-diyl)bis(N,N-dihexylaniline) (dDHADPA), 1,2-bis(4-methoxyphenyl)ethyne (dOMeDPA), DPA, 4,4'-(ethyne-1,2-diyl)dibenzaldehyde (dCHODPA), dimethyl 4,4'-(ethyne-1,2-diyl)dibenzoate (dCOOMeDPA), 4,4'-(ethyne-1,2-diyl)dibenzonitrile (dCNDPA)) were prepared based on the Sonogashira method[47,48] - coupling the respective halogenoarenes with appropriate terminal ethynyl derivatives (procedure A or B, Scheme 2 ESI).

The removal of the trimetylsilane group (TMS) (6c-7c) was made as described in the literature[49] (procedure C), while removal of the - 2-hydroxy-2-methylpropyl group (2c-3c, 8c) was also described in the literature[50,51] (procedure D) (Scheme 2 ESI) (for details see ESI).

2.2 Spectroscopy and fluorescence measurements

Absorption spectra were measured using a Perkin-Elmer Lambda-40P spectrophotometer whereas fluorescence spectra were measured using a FluoroMax-4 (Horriba Yobin-Yvon) spectrofluorimeter. Low temperature luminescence spectra were obtained using an FL-1013 liquid nitrogen dewar assembly.

Fluorescence quantum yields were calculated with: 2-aminopiridine in 0.1 M H_2SO_4 (QY=0.60) (for dOMeDPA, DPA, dCOOMeDPA) and quinine sulphate in 0.5 M H_2SO_4 (QY=0.53±0.02) (for dDMADPA, dDBADPA, dDHADPA, dCHODPA, dCNDPA) as reference and were corrected for the different refractive indices of solvents.

The fluorescence lifetimes were measured with a time-correlated single-photon counting FT300 PicoQuant fluorescence lifetime spectrometer using subnanosecond pulsed diodes: PLS-320 (for DPA, dCHODPA, dCOOMeDPA, dCNDPA) or PLS-340 (for dDMADPA, dDBADPA, dDHADPA).

2.3 Theoretical calculations

All calculations were performed using density functional theory (DFT) within the Turbomole v. 6.4 suite programs on a PC cluster. The structures of all compounds were prepared and initially optimized using the TmoleX program. Energy-minimized structures were located for the ground and the lowest excited states using a B3-LYP hybrid functional with def2-TZVP basis set of triple-ζ quality. This procedure was considered satisfactory if the energy difference between optimized cycles was $<1*10^{-6}$ Hartree for ground state structure optimization and $<1*10^{-7}$ Hartree for excited state structure optimization. In both states, a gradient of $<1*10^{-3}$ au was achieved. The low-lying excited states were treated within the adiabatic approximation of time-dependent density functional theory using a B3-LYP function. The geometry optimization of the excited state was performed using a grid parameter equal to 4. The convergence of all studied systems was checked by

harmonic vibrational analysis. No imaginary frequencies were observed. The rotation energy barriers in the ground and the excited states were calculated by imposing constraints on the dihedral angle formed by the phenyl rings and optimizing the energy of the remaining part of the molecule. In a similar way, the energy of the bent conformation of the molecule in the excited state was calculated by imposing constraints on the one C_{Ph}-C≡C angle and optimizing the remaining part of the molecule under C_s symmetry. A minimum in the potential-energy profiles denotes the energy of the molecule with fully optimized geometry in both ππ* or σπ* states. For a low deformation angle, the calculations were performed in two ways. In the first method, only one C_{Ph}-C≡C angle was changed with constraint to generate energy profiles along this angle and the other one remained unchanged (180 degrees). This method led to the ππ* state ("scorpion-like" structure) (Figs 29 and 32 ESI). In the second approach, two C_{Ph}-C≡C angles were changed at the same time, but constraints were applied only to the one angle whereas the second angle was left free to change during geometry optimization. This led to a planar σπ* (stilbene-type structure) (Figs 30 and 33 ESI). Hence, some differences in the potential energy curve are visible for small deformations of the C_{Ph}-C≡C angle from 180 degrees.

3. Results and discussion

3.1 Absorption spectra

Absorption spectra of the studied compounds were measured in non-polar solvents with different viscosities (cyclohexane, methylcyclohexane (MeCx), hexane, hexadecane), weakly polar 2-methyltetrahydrofurane (MeTHF) and polar acetonitrile (MeCN). Absorption spectra in MeCx are presented in Fig. 2 and for MeTHF and MeCN in Figs 1-2 ESI. The structure of the absorption spectrum of DPA[32,35,39], as well as dDMADPA[28,53] are in agreement with literature data. The absorption spectra of dDBADPA and dDHADPA are the same as the spectrum of dDMADPA. All discussion of the dDMADPA spectra also refers to these two derivatives. For DPA derivatives, the substituents in positions 4 and 4` of the phenyl ring cause a red shift in the absorption spectrum compared to the parent compound. The greatest shift is observed for the di-N,N-dimethyl (DMA) substituent (λ=345.5 nm) compared to DPA (λ=298 nm). The first vibronic lines of the long-wave absorption band are summarized in Table 1.

Table 1. The position of the long wavelength vibronic band and main vibrational mode of 4,4`-phenylacetylene derivatives in MeCx.

Substituent of di-phenytlacetylene derivative	λ /nm	$\nu_{C\equiv C}$ / cm^{-1}
-H	298	2080
-OMe	312.5	2043
-CN	321.5	2063
-COOMe	325	2012
-CHO	337	2002
-DMA	345.5	1968

For all studied molecules, the single progression of the most prominent

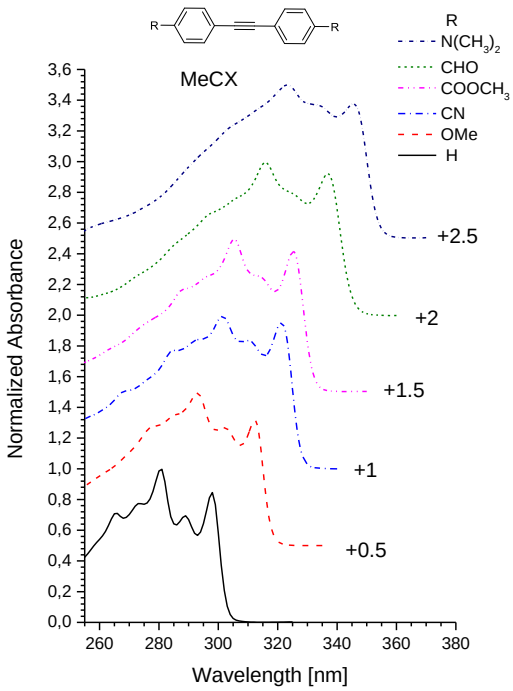

Fig 2. Normalized absorption spectra of symmetrically substituted diphenylacetylene derivatives in MeCx.

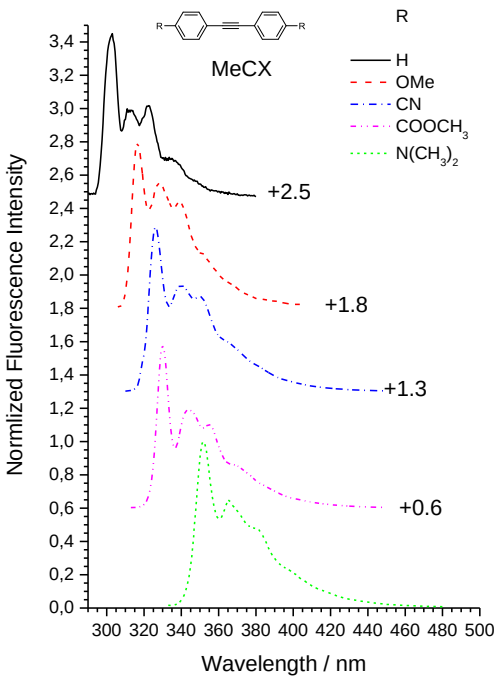

Fig 3. Normalized fluorescence spectra of symmetrically substituted diphenylacetylene derivatives in MeCx.

vibronic structure of about 2000-2100 cm^{-1} is displayed from the origin that has been assigned to the C≡C stretching mode[39]. Moreover, other vibronic bands (about 1000 cm^{-1}) are visible in the absorption spectrum, which may be attributed to the total symmetric vibrations of the phenyl ring[39]. Both progressions are clearly visible for all the studied derivatives, however, for dCHODPA and dDMADPA they are broadened. Absorption spectra measured in hexane, cyclohexane and hexadecane are very similar to spectra measured in MeCx and are not presented here. The polarity of the solvent has practically a minor influence on the position of the absorption spectrum. Changing a solvent from non-polar MeCx to more polar MeTHF, did not cause significant changes in the shape of the long-wavelength absorption band (Table 1, ESI). However, in polar acetonitrile, the shape of the absorption band of dCHODPA and dDMADPA undergoes slight changes due to a loss of vibronic structure associated with the vibration of the phenyl ring, in agreement with data published by Rosspeinter et al.[28] and Onitsch et al.[53] (Fig. 2 ESI). Additionally, in acetonitrile, a small blue-shift absorption spectra are observed, except for dDMADPA, whose spectrum is slightly shifted to the red (Table 1, ESI).

3.2 Room temperature fluorescence

Fluorescence spectra of DPA derivatives in MeCx are presented in Fig. 3. The fluorescence spectrum of DPA (tolane) is in accordance with previously published data[32,35,39]. In all presented fluorescence spectra, a progression of the frequency at about 2100 cm^{-1} is displayed from the origin and vibronic band with about 1100 cm^{-1}, which may be assigned to the vibration of phenyl rings. The substituents do not change the shape of the emission spectra, however, a red shift is observed in comparison to the DPA spectrum. The lowest energy vibronic band in MeCx is located at 304 nm for DPA, 316.5 nm for dOMeDPA, 326 nm for dCNDPA, 330 nm for dCOOMeDPA and 352 nm for dDMADPA[28,53]. All DPA derivatives in non-polar or weakly polar solvents possess characteristic emission band shapes that are not a mirror symmetry of the absorption spectrum. Such phenomena occurs also for the arylethynyl derivatives of DMA[12,19], as well as for phenylene ethynylene oligomers[22,25,26,28,54], and have been explained in terms of torsional disorder and quadratic coupling between the ground and the first excited state[55] or the exciton model developed by Liu et al.[56,57].

The polarity of the solvents used in the study had little effect on the position of the emission spectra of the studied compounds. The first vibration band changes its position by about 2 nm going from non-polar MeCx to polar MeCN - regardless of the type of substituent on the phenyl ring. The exception is dDMADPA, which shows a clear solvatochromic effect[28]. For this derivative, the first emission band moves to 359.5 nm and 367.5 nm in MeTHF and acetonitrile, respectively (Table 2, ESI). The polarity of the solvent has a greater impact on the fluorescence band shape, especially for dOMeDPA, dCOOMeDPA and dDMADPA, for which the vibronic structure of the emission spectrum becomes broader with increasing solvent polarity (Figs 3 and 4, ESI).

The fluorescence quantum yields of DPA derivatives are gathered in Table 3 ESI. dCHODPA is not fluorescent at all. Among the studied compounds, the derivatives containing the electron-accepting group (nitrile or ester) are characterized with the greatest fluorescence quantum yield of about 30%, while those containing an electron-donating group (methoxy or N,N-dialkylamino) are weakly fluorescent. Their fluorescence quantum yields are comparable to, or a little higher than, the fluorescence quantum yield of DPA[35] and for dDMADPA it is comparable to the data published by Rosspeintner et al.[28]. The elongation of the alkyl substituent on the nitrogen atoms of amino derivatives of diphenylacetylene (dDBADPA, dDHADPA), does not increase the fluorescence quantum yield, for which the values are comparable to dDMADPA. The fluorescence quantum yields of dDHADPA measured by ourselves are one order lower than those published by Liu et al.[58]. Fluorescence quantum yields were also measured in other solvents with different viscosities (cyclohexane, hexane and hexadecane) and are gathered in Table 3 ESI. Slightly higher fluorescence quantum yields were measured in hexadecane (viscosity 3.04 mPa*s), in comparison to hexane (viscosity 0.292 mPa*s), however, the differences in fluorescence quantum yields is in the range of experimental error. Thus, it is not possible to unambiguously come to a conclusion regarding the influence of viscosity of solvent on the fluorescence quantum yield. It seems, that the partial inhibition of the mutual rotation of the phenyl rings by elongation of substituents on the nitrogen atom or increase of solvent viscosity does not affect the photophysical processes, indicating a low energy barrier of phenyl ring rotation. Thus, the studied compounds cannot be used as viscosity probes[59].

A certain explanation for the low fluorescence quantum yield of derivatives with electron-donating groups, in comparison with those possessing electron-withdrawing groups, can be drawn by analysing the fluorescence excitation and absorption spectra. The fluorescence excitation spectra of dCOOMeDPA (Fig. 4, Figs 5,6, ESI) or dCNDPA (Figs 9-11, ESI) in all studied solvents superimposed on one another, whereas for dOMeDPA (Fig. 5, Figs 7,8, ESI) a substantial difference between them can be seen. Fluorescence excitation spectrum of the dOMeDPA derivative exhibits a very clear decrease in the intensity for wavelengths shorter than 310 nm excitation in all studied solvents (Fig. 5 and Figs 7,8 ESI), similarly to that observed for DPA in hexane solution[32]. The differences between the absorption and fluorescence excitation spectrum are also present for dDMADPA (Figs 12-14, ESI), although much less pronounced than that for dOMeDPA.

The sudden collapse of the fluorescence excitation spectrum, would be the consequence of extra nonradiative processes connected with the thermal deactivation of S_1 (1^1B_{1u}) state to the 1^1Au state with $\sigma\pi^*$ character, which becomes the lowest excited singlet state[34,35,43-45]. Probably this is the reason for low values of fluorescence quantum yield of derivatives containing electron-donating substituents compared to the derivatives with electron-withdrawing ones. Because of the low values of fluorescence quantum yield of dOMeDPA, fluorescence lifetimes were measured only for dCNDPA, dCOOMeDPA and dDMADPA derivatives (Table 4 ESI). For these derivatives, the fluorescence intensity decay is mono-exponential in all studied solvents, except for dDMADPA. The fluorescence lifetimes of dCNDPA and dCOOMeDPA are very similar and are in the range of 640 to 700 ps (Table 4 ESI). These values are comparable to the fluorescence lifetime of DPA (0.6 ns) measured in MeCx at 77 K by Nagano et al.[39], as well as of the fluorescence lifetime of mono-substituted CNDPA and COOMeDPA for which the fluorescence intensity shows a single exponential decay with a lifetime of several hundred picoseconds[60]. Moreover, both the fluorescence quantum yield and fluorescence decay time of dCNDPA measured by

ourselves are smaller than those estimated by Hirata et al.[61] ($\varphi \approx 0.5$, $\tau \approx 1.1$ ns).

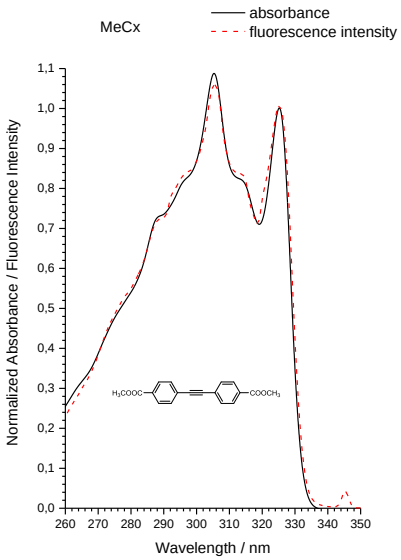

Fig 4. Absorption (black solid line) and fluorescence excitation spectrum (red dashed line) of dCOOMeDPA in MeCX

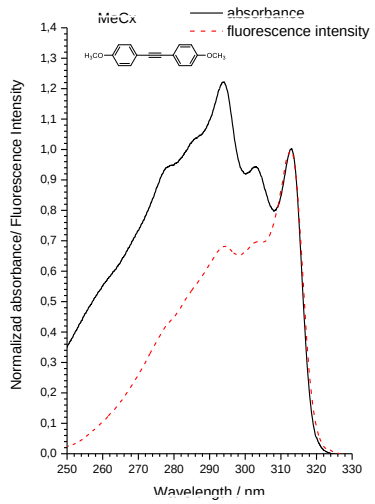

Fig 5. Absorption (black solid line) and fluorescence excitation spectrum (red dashed line) of dOMeDPA in MeCX.

The fluorescence intensity decay of dDMADPA is bi-exponential with very short (tens of picosecond) and longer (sub-nanosecond) lifetimes (Table 4 ESI). It should be noted, due to the relatively large half-width of our excitation pulse, that the short decay time is poorly defined. A bi-exponential fluorescence intensity decay with one very short (a few picoseconds) and one longer (hundreds of picoseconds) component was also determined by Hirata et al.[62] for mono-substituted aminophenyl-phenylacetylene in hexane at room temperature.

3.3 Luminescence at 77 K

Low temperature (at 77 K) luminescence and excitation spectra of the studied compounds were measured in two solvents (MeCx and MeTHF) and compared with fluorescence spectra measured at room temperature. The emission spectra of dOMeDPA and dCNDPA in MeCx are presented in Figs 6 and 7, respectively, whereas the spectra for the remaining compounds are given in Figs 15-22, ESI. In contrast to the room temperature results, almost mirror symmetric images between the fluorescence and fluorescence excitation spectra are recognizalbe at 77 K. This indicates a hindered ring torsion angle in the MeCx and MeTHF organic glass. For all the studied compounds, the fluorescence intensity is much more intense than phosphoresence indicating a low intersystem crossing rate constant. For DPA, both the fluorescence excitation and emission spectra, as well as the phosphorescence spectrum, are the same as published by Nagano et al.[39]. In MeTHF, the glass spectra are not different to those measured in MeCx glass, except for the phosphorescence intensity, which is higher in MeTHF than in MeCx for all the studied compounds, although it is not clearly visible for all of the compounds. For DPA, a large difference in the fluorescence intensities measured at 77K and at room temperature is observed (Fig 21,22, ESI). This is consistent with the results published by Ferrante et al.[35] who measured the fluorescence quantum yield as 0.5 and $3.36*10^{-3}$ in a 3-methylpentane at 77 K and at room temperature, respectively. Similarly to DPA, also for dOMeDPA (Fig. 6, Fig. 15, ESI), a substantial increase of fluorescence intensity at 77 K, compared to room temperature, is recorded in both solvents. A significant increase of fluorescence intensity, although smaller than for DPA and dOMeDPA, was observed for dDMADPA with, only very weak phosphorescence (Figs 17,18, ESI), whereas for dCNDPA (Figs 7, 16 ESI) and dCOOMeDPA (Figs 19, 20, ESI) the lowest increase of fluorescence intensity with decreasing temperature is observed. For dCHODPA, which is not fluorescent in liquid solution, only a very weak phosphorescence at about 500 nm is observed (data not shown). The results presented above indicate a substantial influence of the type of substituents and temperature on the photophysical properties of DPA derivatives. A substantial increase of fluorescence intensity at 77 K of DPA and its derivatives possessing electron-donating substituents indicate the exclusion of a non-radiative transition associated with the transition to the dark $\sigma\pi^*$ state in the rigid environment. However, for dCOOMeDPA and dCNDPA, the lack of substantial changes of fluorescence intensity with decreasing temperature demonstrates that such a transition is already excluded at room temperature. Thus, the temperature dependence of fluorescence intensity in an elegant way confirms, the results obtained from transient absorption spectroscopy and theoretical calculations, that the $\sigma\pi^*$ state is the lowest excited state for DPA and its derivatives with an electron-donating substituent while it is the $\pi\pi^*$ state for derivatives with an electron-withdrawing substituent[37,43,45,60-62].

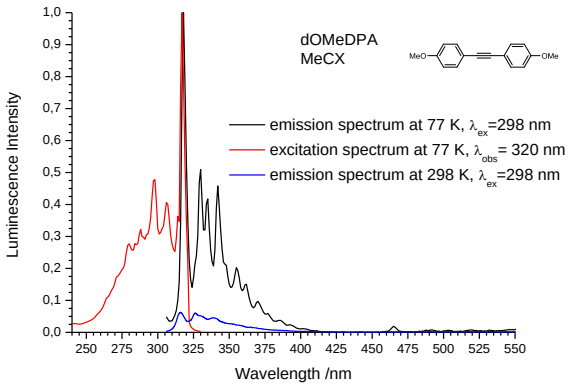

Fig. 6. The luminescence spectrum (black line), fluorescence excitation spectrum (red line) at 77 K and room temperature fluorescence spectrum (blue line) of dOMeDPA in methylcyclohexane.

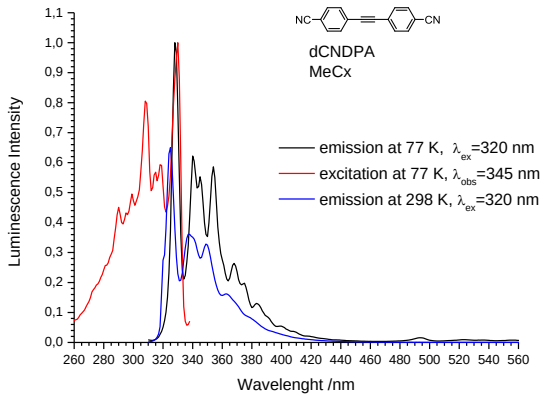

Fig. 7. The luminescence spectrum (black line), fluorescence excitation spectrum (red line) at 77 K and room temperature fluorescence spectrum (blue line) of dCNDPA in methylcyclohexane.

3.4 Theoretical calculations

The optimized geometry was found to be planar with D_{2h} symmetry in both, the ground and excited states. The triple-bond length of the optimized DPA structure in the ground state (1.209 Å) was comparable to that computed by others (1.216 Å)[39] (1.22 Å)[43] (1.200 Å)[35] and determined from a crystallographic structure (1.206 Å)[40]. The type of substituent has a minor influence on the triple-bond length, which slightly shortens with an increase in the electron-withdrawing strength of the substituent (Table 5 ESI). The lack of mirror symmetry between the absorption and emission spectra in liquid solution indicates a low energy barrier of rotation of DPA and its derivatives in the ground state. To understand the influence of substituents in the phenyl ring on torsional motions, we studied the torsional potential in both the ground and excited states within the framework of the local mode approximation using a DFT method. Fig. 23, ESI presents DFT-based torsional potentials for dOMeDPA in the ground and excited states. As the torsional potentials for the remaining compounds have the same shape, they are not presented. The torsional potential in the ground state is well approximated by a simple periodic potential of the form:

$$V(\Theta) \quad \frac{V_{max}}{2}(1-\cos 2\Theta) \qquad (1)$$

where: V_{max} is the barrier height of the torsional potential and θ is the ring-to-ring torsional angle. The barrier heights of the torsional potential calculated using the above equation, for all the studied compounds, are gathered in Table 6, ESI. The energy barriers of rotation in the ground state are in the range 3.6 kJmol^{-1} for dOMeDPA to 4.5 kJmol^{-1} for dCHODPA. For DPA, the barrier energy of rotation (3.8 kJmol^{-1}) is comparable to the value (3.3 kJmol^{-1}) calculated by Li et al.[41]. However, the experimentally determined energy barrier is lower than the theoretically calculated value for DPA (2.5 kJmol^{-1})[31,54]. For compounds possessing electron-donating substituents, the energy barriers of rotation in the ground state are a little lower than those for electron-withdrawing substituents. The rate constant of the conversion through the energy barrier during the rotation can be calculated on the basis of transition-state theory using the equation:

$$k_{c\to c'} = \left(\frac{\kappa T}{h}\right) * e * \exp(\Delta S/R) * \exp(-\Delta E_a / RT) \qquad (2)$$

where: k is the Boltzmann constant, T is the absolute temperature, h is Planck`s constant, R is the gas constant, ΔS is the entropy change, and ΔE_a is the energy of activation. It is difficult to assign a value to the transmission coefficient, κ, which incorporates all correction factors and uncertainties. We chose, κ=0.4 as for ring inversion[63] and ΔS=0 and for these values the rate constant and rotamer lifetime were calculated. At room temperature, and for the energy barrier of rotation equal to 4 kJmol^{-1}, the rate constant of rotation is 1.35*10^{12} s^{-1}, which gives the rotamer lifetime equal τ=1/k=740 fs, which is tantamount with the free rotation in the ground state (RT≈2.5 kJmol^{-1}). Although DFT gives overestimated values to the energy barrier of rotation[64], the results show a slight influence of the type of substituent on the value of the rotation barrier in the ground state. A simple periodic potential (eq. 1) poorly describes the torsional potential in the excited state, which however, can be approximated using the Gauss function (Fig. 23, ESI). The energy barrier of rotation in the excited state is about one order higher than in the ground state indicating a hampered phenyl ring rotation in the excited state, which is attributed to the breaking of the cylindrical structure of the electron density along the axis of symmetry[54]. The energy barriers of rotation in the excited state (Table 7, ESI), are in the range of 30 kJmol^{-1} for DPA to 36.6 kJmol^{-1} for dOMeDPA and similar to that of 1,4-bis(phenylethynyl)benzene[64]. Moreover, there is no correlation of the type of substituent and height of energy barrier of rotation. For an energy barrier equal to 30 kJmol^{-1}, the calculated rate constant of rotation is k=3.76*10^7 s^{-1} and the rotamer lifetime is τ=26.6 ns while for ΔE=36.6 kJmol^{-1}, k=2.62*10^6 s^{-1} and the rotamer lifetime is τ=382 ns. Thus, during the fluorescence lifetime of DPA derivatives, which are about 0.6 ns, no rotation will take place in the excited state. It is worth noting that for the dCHODPA derivative, the energy barrier of rotation is about half lower (12.7 kJmol^{-1}) than for the other studied derivatives and the torsional potential in the excited state can be well described using eq. 1. The calculated rate constant of rotation for dCHODPA is k=4.03*10^{10} s^{-1} and τ=24.8 ps. This indicates a fairly free rotation of the phenyl ring in the excited state. However, as in the case of the ground state, the energy barrier of rotation in the excited state seems to be overestimated. In the ππ* excited state, the height of the rotation barrier for DPA

(19.1 kJmol^{-1}) estimated by Okuyama et al.[31] from fluorescence jet spectroscopy is substantially lower than that calculated by ourselves (29.8 kJmol^{-1}) using the DFT method. Taking into account experimentally determined value of rotation energy barrier (19.1 kJmol^{-1}), the DPA rotamer lifetime in the excited state is equal to 316 ps, and therefore comparable to the fluorescence lifetime. Thus, rotation in the excited state may provide an additional radiationless channel for excited state deactivation. However, it does not explain the difference in the fluorescence quantum yield between the symmetrical derivatives of DPA containing electron-donating or electron-withdrawing substituents.

As suggested by Zgierski et al.[43,45], the loss of fluorescence in jet-cooled DPA that occurs at an excitation energy slightly above the electronic origin of the fluorescent ππ* state, and other unusual photophysical properties of DPA, could be explained by the crossings of the ππ* and dark σπ* state that arise from the promotion of an electron from the phenyl π orbital to the σ* localized in the acetylene unit. From an analysis of the orbital energies, calculated for the optimized ground state geometry, for mono-substituted DPA derivatives containing electron-withdrawing substituents (nitrile or methyl ester), the authors concluded that the presence of an electron-withdrawing substituent leads to an increase in the energy of the σπ* state and shift in the intersection of the ππ*/σπ* states to higher energy, causing the state switch from linear ππ* to bent σπ* to be highly ineffective. For derivatives containing electron-donating substituents (dOMeDPA, dDMADPA), the opposite effect was obtained. The calculations also predict the occurrence of a strongly allowed absorption from the lowest energy σπ* state to a higher lying σπ* state for electron-donating derivatives and the lack of such an absorption for electron-withdrawing derivatives. That conclusion explains the long-wavelength absorption (700 nm and above) recorded by femto- and picosecond transient absorption spectroscopy for mono-substituted[43] and di-substituted[37,61] derivatives of DPA.

The potential-energy profiles of low-lying electronic states as a function of bent (C_{Ph}-C≡C) angle for DPA and its symmetrical derivatives were studied using the DFT/B3LYP/def2TZVP method in order to estimate the influence of the character of substituents on the energy of low lying excited states. For all studied derivatives, the planar structure with linear geometry (C_{Ph}-C≡C angle 180 degrees) is most stable with a C≡C bond length about 1.24 Å - a little longer than in the ground state (1.21 Å). Moreover, the C_{Ph}-C bond length is about 1.38 Å (Table 5 ESI). The potential-energy profiles for DPA derivatives containing electron-donating (dOMeDPA) or electron-accepting (dCNDPA) substituents are presented in Figs 8 and 9, respectively, and in Figs 24-27, ESI for the other studied compounds.

The energy barrier (ΔE) and bent angle for the σπ*/ππ* state crossing, energy of stabilization (ΔE_{stab}) for fully optimized structure in σπ* and ππ* states and values of bent angle of lowest energy structure in the appropriate state are gathered in Table 2.

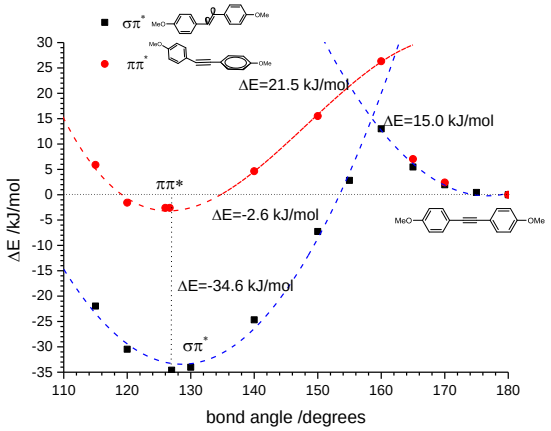

Fig. 8. The potential-energy profiles as a function of C_{Ph}-C≡C bending angle for dOMeDPA - DPA derivative containing an electron-donating substituent.

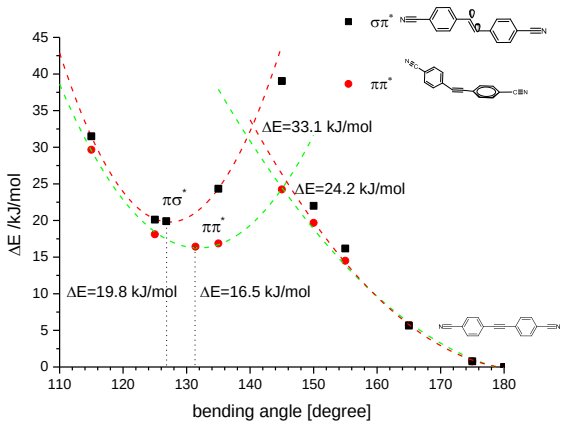

Fig. 9. The potential-energy profiles as a function of C_{Ph}-C≡C bending angle for dCNDPA - DPA derivative containing an electron-accepting substituent.

Table 2. The energy barrier (ΔE) and bent angle for the σπ*/ππ* state crossing, energy of stabilization (ΔE_{stab}) for fully optimized structure in σπ* and ππ* states and values of bent angle of lowest energy structure in the appropriate state.

Derivative of DPA	Energy barrier (ΔE) of σπ*/ππ* state crossing / Jmol^{-1}	Bent angle for σπ*/ππ* state crossing / degree	Energy stabilization (ΔE_{stab}) of σπ* state /kJmol^{-1}	Bent angle for lowest energy structure in σπ* state	ΔE_{stab} of ππ* kJmol^{-1}	Bent angle for lowest energy structure in ππ* state
DPA	14.65	155.0	-21.5	127.5	-5.04	128.8
dOMeDPA	15.0	158.5	-34.6	126.7	-2.60	127.0
dDMADPA	27.4	157.5	-23.5	126.7	2.46	126.9
dCNDPA	31.3	140.0	19.8	126.7	16.5	131.4
dCOOMeDPA	35.0	140.0	24.3	126.6	18.4	131.8
dCHODPA	44.5	138.0	36.0	126.5	-	-

The results presented above fully support the conclusions drawn from transient absorption spectroscopy for mono-substituted, as well as for symmetrically substituted, DPA derivatives. For DPA, the dOMeDPA and dDMADPA σπ* state is the lowest excited state whereas the ππ* state is the lowest excited state for dCNDPA and dCOOMeDPA. Taking the energy of the fully optimized planar linear structures in the excited state as references, the σπ* energy stabilization is about -21.5 kJmol^{-1} for DPA, -23.5 kJmol^{-1} for dDMADPA and -34.6 kJmol^{-1} for dOMeDPA (Table 2). For electron-withdrawing derivatives, the linear planar structure has the lowest energy. The σπ* state is destabilized and the energy of destabilization is equal to 19.8 kJmol^{-1} for dCNDPA, 24.3 kJmol^{-1} for dCOOMeDPA and 36 kJmol^{-1} for dCHODPA. The bent C_{Ph}-C≡C angle for the lowest energy structure in the σπ* state is approximately the same for all studied derivatives and equal to 127 degrees. The bond length between the C2 and C3 atoms (acetylenic unit) is in the range 1.34 to 1.35 Å, while between the aromatic carbon and acetylenic unit it is 1.42 Å (Table 5 ESI). For electron donating substituents, the energy of the fully optimized "scorpion-like" structure in the ππ* state is lower than that of the linear planar structure. The energy of stabilization is -5.04 kJmol^{-1} for DPA and -2.60 kJmol^{-1} for dOMeDPA. However, the "scorpion-like" structure of dDMADPA, has a higher energy (ΔE_{stab}=2.46 kJmol^{-1}) than the planar linear structure. For derivatives containing electron-withdrawing substituents, the planar linear structure is the most stable one. The energy of destabilization for the bent structure of dCNDPA and dCOOMeDPA in the ππ* state is equal to 16.5 kJmol^{-1} and 18.4 kJmol^{-1}, respectively. Additionally, for the two last-mentioned compounds, the bent ππ* state has a lower energy than the bent planar structure in the σπ* state. The energy gap between the ππ* and σπ* bent states are rather low (6 kJmol^{-1} for dCOOMeDPA and 3.3 kJmol^{-1} for dCNDPA). Surprisingly, the aldehyde derivative of DPA does not show any additional minima on the potential energy curve for the ππ* state (Fig 27, ESI=. The "Scorpion-like" structures in the ππ* states are characterized by shorter triple bonds than linear ones (Table 5 ESI). The accurate determination of the intersection of the σπ* and ππ* states is difficult due to the approximations of the potential energy curve by the second order polynomial function because of the limited number of points. The lowest energy barrier for state-crossing was obtained for DPA and dOMeDPA (about 15 kJmol^{-1}) and for dDMADPA (27 kJmol^{-1}). The highest values were obtained for electron-withdrawing derivatives, 31.3 kJmol^{-1}, 35 kJmol^{-1} and 44.5 kJmol^{-1} for dCNDPA, dCOOMeDPA and dCHODPA, respectively. Moreover, the lowest value of C_{Ph}-C≡C angle deformation from the linear structure required to achieve the σπ*/ππ* states intersection is obtained for DPA and its electron-donating derivatives (from 155 degrees for DPA to 158.5 degrees for dOMeDPA) and highest for electron-withdrawing derivatives (about 140 degrees) (Table 2), which is consistent with the suggestion of Zgierski et al.[43,45]. The calculated value of the barrier of state crossing for DPA (14.65 kJmol^{-1} which corresponds to 1225 cm^{-1}) is lower than that theoretically calculated by Zgierski et al.[43] (0.29 eV; 2339 cm^{-1}), and higher than that resulting from the jet-cooling fluorescence data (750 cm^{-1})[31,34] or temperature dependence of transient absorption spectroscopy in the condensed phase (940 cm^{-1} in methylcyclohexane)[32]. However, it is close to the value obtained from the temperature dependence of fluorescence quantum yield in 3-methylpentane (14 kJmol^{-1})[35]. A similar value for the energy barrier of states intercrossing was obtained for dOMeDPA (15 kJmol^{-1}; 1225 cm^{-1}), which is comparable to the 830 cm^{-1} obtained from the temperature dependence of transient absorption spectroscopy in non-polar solvents[61]. The energy barrier of the states crossing can be estimated from the comparison of the absorption and fluorescence excitation spectra. The increase of excess of excitation energy above the 0-0 band causes the decrease of fluorescence yield for both DPA[32] and dOMeDPA (Fig. 5). For dDMADPA, the energy barrier of states crossing is about two times higher than that for DPA and dOMeDPA (27.4 kJmol^{-1}; 2290 cm^{-1}), however, the lack of additional experimental data does not allow for the verification of this value. Comparing the excitation fluorescence spectrum with the absorption spectrum of dDMADPA, it is difficult to see a significant decrease of fluorescence intensity with the excess of excitation energy (Figs 17,18, ESI), which may indicate a rather high energy barrier. For the mono-substituted amino-DPA, the energy activation of states intercrossing was estimated to be 600 cm^{-1} in hexane solution[62]. For the DPA derivatives containing electron-withdrawing substituents, the intercrossing of the σπ*/ππ* states energy barrier is much higher, higher than the energy of transitions between the linear and bent structures of the ππ* states (Figs 8, 24, ESI). For these derivatives, the fluorescence quantum yield is high (except for dCHODPA) and, the fluorescence excitation spectrum coincides with the absorption spectrum. Moreover, the transient absorption spectra lack the long-wavelength transition corresponding to the transition σπ*←σπ*[60]. Thus, they do not show any anomalous dynamic behaviour but act as typical aromatic compounds.

4. Conclusions

Diphenylacetylene (DPA) and its symmetrically substituted derivatives containing electron-donating (N,N-dimethyl, methoxy) or electron-accepting (nitrile, ester or aldehyde) substituents were studied using spectroscopic and theoretical methods. It was found that substituents do not change the structure of the absorption and fluorescence spectra compared to that of DPA. However, substituents shift both the absorption and fluorescence spectra toward the longer-wavelengths. For electron-donating derivatives, blurred vibronic structures are observed. Based on the emission spectra measured at room and liquid nitrogen temperature, it can be stated that for derivatives of DPA containing electron-donating substituents that the fluorescence intensity strongly depends on temperature in contrast to derivatives possessing electron-accepting substituents. Theoretical calculations show that the energy barrier of rotation in the ground state is low while it substantially increases in the excited state. These results explain the lack of symmetry between the excitation and the absorption spectra measured at room temperature and symmetry of the spectra in organic glass. Furthermore, calculations showed, that the lowest excited state for DPA and its symmetrical derivatives containing amino or methoxy substituents is the σπ* state, whereas for nitrile, ester or aldehyde derivative it is the ππ* state - in agreement with the suggestion of Zgierski et al.[43,45] for mono-substituted DPA derivatives. Thus, the results obtained from fluorescence spectroscopy are fully consistent with the conclusions drawn from femto- and picosecond transient absorption spectroscopy of mono- and di-substituted DPA derivatives.

Acknowledgements

This work was financially supported under grant UMO-2011/01/B/ST4/06094 from National Science Center (NCN).
The publication is financed from European Social Fund as a part of the project "Educators for the elite – integrated training program for PhD students, post-docs and professors as academic teachers at University of Gdansk" within the framework of Human Capital Operational Programme, Action IV. This publication reflects the views only of the author, and the funder cannot be held responsible for any use which may be made of the information contained therein.

Notes and references

Faculty of Chemistry, University of Gdańsk, Wita Stwosza 63, Poland
*wieslaw.wiczk@ug.edu.pl

† Electronic Supplementary Information (ESI) available. See DOI: 10.1039/b000000x/

1 1. D.T. McQuade, A. E. Pullen, T. M. Swager, *Chem. Rev*., 2000, **100**, 2537-2574.

2. 2. S. Günes, H. Neugebaueer, N. S. Sariciftci, *Chem. Rev*., 2007, **107**, 1324-1338.

3. M. Kivala, F. Diederich, *Acc. Chem. Res*., 2009, **42**, 235-248.

4. U. H. F. Bunz, *Chem. Rev*., 2000, **100**, 1606-1644.

5. K. Kuroda, T. M. Swager, *Chem. Commun*., 2003, 26-27.

6 6. P.F. van Hutten, J. Wideman, A. Meetsma, G. Hadziioannou, *J. Am. Chem. Soc*., 1999, **121**, 5910-5918.

7. T. Goodson, W. Li, A. Gharavi, L. Yu, *Adv. Matter*., 1997, **9**, 639-643.

8 8. S. Pan, Q. Fu, T. Huang, A. Zhao, B. Wang, Y. Luo, J. Yang, J. Hou, *Proc. Natl. Acad. Sci. USA*, 2009, **106**, 1559-1563.

9 9. A. Facchetti, *Chem. Mater*, 2011, **23**, 733-758.

10. T. Y. Chu, J. Lu, J. Ding, Y. Tao, *J. Am. Chem. Soc*., 2011, **133**, 4250-4253.

11 11. B. Carlotti, R. Flamini, A. Spalletti, A. Marrocchi, F. Elisei, *ChemPhysChem*, 2012, **13**, 724-735.

12 12. R. Flamini, I. Tomasi, A. Marrocchi, B. Carlotti, A. Spalletti, *J. Photochem. Photobiol. A:Chem*., 2011, **223**, 140– 148.

13 13. T.-I Ho, A. Elangovan, H.-Y. Hsu, S.-W. Yang, *J. Phys. Chem. B*, 2005, **109**, 8626-8633.

14. S.-W. Yang, A. Elangovan, K.-C. Hwang, T.-I. Ho, *J. Phys. Chem. B*, 2005, **109**, 16628-16634.

15. A. Elangovan, K.-M. Kao, S.-W. Yang, Y.-L. Chen, T.-I. Ho, Y. O. Su, *J. Org. Chem*., 2005, **70**, 4460-4469.

16. A. Elangovan, H.-H. Chiu, S.-W. Yang, T.-I. Ho, *Org. Biomol. Chem*., 2004, **2**, 3113-3118.

17. A. Elangovan, T.-Y. Chen, C.-Y. Chen, T-I. Ho, *Chem. Commun*., 2003, **17**, 2146-2147.

18. A. Elangovan, J.-H. Lin, S.-W. Yang, H.-Y. Hsu, T.-I. Ho, *J. Org. Chem*., 2004, **69**, 8086-8092.

19. U. Subuddhi, S. Haldar, S. Sankararaman, A. K. Mishra, *Photochem. Photobiol. Sci*., 2005, **5**, 459-466.

20. A. D. Malakhov, M. V. Skorobogatyi, I. A. Prokhorenko, S. V. Gantarev, D. T. Kozhich, D. A. Stetsenko, I. A. Stepanova, Z. O. Shenkarev, Y. A. Berlin, V. A. Korshun, *Eur. J. Org. Chem*., 2004, **6**, 1298-1307.

21. H. Nakayama, S. Kimura, *J. Org. Chem*., 2009, **74**, 3462-3468.

22. G. Duvanel, J. Grilj, A. Gossauer, E. Vauthley, *Photochem. Photobiol. Sci*., 2007, **6**, 956-963.

23. R. M. Adhikari, D. C. Neckers, B. Shah, *J. Org. Chem*., 2009, **74**, 3341-3349.

24. J. G. Rodrigez, J. L. Tejedor, *Tetrahedron*, 2005, **61**, 3033-3043.

25. P. V. James, P. K. Sudeep, C. H. Suresh, K. G. Thomas, *J. Phys. Chem*., 2006, **110**, 4329-4337.

26. A. Beeby, K. S. Findlay, A. E. Goeta, L. Porres, S. R. Rutter, A. L. Thompson, *Photochem. Photobiol. Sci*., 2007, **6**, 982-986.

27. B. Liu, H.-Q. Wang, Y.-D. Zhao, Z.-L. Huang, *J. Mol. Struc*., 2007, **833**, 82-87.

28. A. Rosspeinter, G. Angulo, C. Onitsch, M. Kivala, F. Diederich, G. Grampp, G. Gescheidt, *Chem. Phys. Chem*., 2010, **11**, 1700-1710.

29. A. Beeby, K. Findlay, P. L. Low, T. B. Marder, *J. Am. Chem. Soc*., 2002, **124**, 8280-8284.

30. M. Levitas, K. Schmeider, H.Ricks, K. D. Shimizu, U. H. F. Bunz, M. A. Gracia-Garibay, *J. Am. Chem. Soc*., 2001, **123**, 4259-4265.

31. K. Okuyama, T. Hasegawa, N. Mikami, *J. Phys. Chem*., 1984, **88**, 1711-1716.

32. Y. Hirata, T. Okada, N. Mataga, T. Nomoto, *J. Phys. Chem*., 1992, **96**, 6559-6563.

33. C. Adamo, D. Jacquemin, *Chem. Soc. Rev*., 2013, **42**, 845-856.

34. M. Gutmann, M. Gudipati, P.-F. Schonzart, G. Hoheneicher, *J. Phys. Chem*., 1992, **96**, 2433-2442.

35. C. Ferrante, U. Kensy, B. Dick, *J. Phys. Chem*., 1993, **97**, 13457-13463.

36. T. Ishibanshi, H. Hamaguchi, *J. Phys. Chem. A*, 1998, **102**, 2263-2269.

37. Y. Hirata, *Bull. Chem. Soc. Jpn*., 1999, **72**, 1647-1664.

38. T. Ishibashi, H. Okamoto, H. Hamaguchi, *Chem. Phys. Latt*., 2000**, 325**, 212-218.

39. Y. Nagano, T. Ikoma, K. Akiyama, S. Tero-Kubota, *J. Am. Chem. Soc*., 2003, **125**, 14103-14112.

40. R. Thomas, S Lakshmi, S. K. Pati, G. U. Kulkarni, *J. Phys. Chem. B*, 2006, **110**, 24674-24677.

41. Y. Li, J. Zhao, X. Yin, H. Liu, G. Yin, *Phys. Chem. Chem. Phys*., 2007, **9**, 1186-1193.

42. P. W. Thulstrup, S. V. Hoffmann, B. K. V. Hansen, J. Spanget-Larsen, *Phys. Chem. Chem. Phys*., 2011, **13**, 16168-16174.

43. M. Z. Zgierski, E. C. Lim, *Chem. Phys. Lett*., 2004, **393**, 143-149; 352-355

44. S. Thorwirth, M. E. Harding, D. Muders, J. Gauss, *J. Mol. Spectr*., 2008, **251**, 220-223.

45. M. Z. Zgierski, T. Fujiwara, E. C. Lim, *Acc. Chem. Res*., 2010, **43**, 806-817.

46. C. Monnereau, E. Blart, F. Odobel, *Tetrahedron Lett*., 2005, **46**, 5421-5423.

47. K. Sonogashira, *J. Organomet. Chem*., 2002**, 653**, 46-49.

48. K. Sonogashira, Y. Tohda, N. Hagihara, *Tetrahedron Lett*., 1975, **16**, 4467-4470.
49. A. de Meijere, S. Kozhuskov, T. Haumann, R. Boese, C. Puls, M. J. Cooney, L. T. Scott, *Chem. Eur. J*., 1995, **1**, 124-131.
50. G. Rodriguez, J.L. Tejedor, T. La Parra, C. Díaz, *Tetrahedron*, 2006, **62**, 3355-3361.
51. Q. Xiao, R.T. Ranasinghe, A.M.P. Tang, T. Brown, *Tetrahedron*, 2007, **63**, 3483-3490.
52. A. Elangovan, Y. H. Wang, T.-I. Ho, *Org. Lett*. 2003, **5**, 1841-1844.
53. 53. C. Onitscg, A. Rosspeinter, G. Angulo, M. Griesser, M. Kivala, B. Frank, F. Diederich, G. Gescheidt, *J. Org. Chem*., 2011, **76**, 5628-5635.
54. S. Toyota, *Chem. Rev*., 2010, **110**, 5398-5424.
55. 55. M. I. Sluch, A. Godt, U.H.F. Bunz, M.A. Berg, *J. Am. Chem. Soc*., 2001, **123**, 6447-6448.
56. 56. L.T. Liu, D. Yaron, M.I. Sluch, M.A. Berg, *J. Phys. Chem. B*, 2006, **110**, 18844-18852.
57. L.T. Liu, D. Yaron, M.A. Berg, *J. Phys. Chem. C*, 2007, **111**, 5770-5782.
58. B. Liu, J. Liu, H.-Q. Wang, Y.-D. Zhao, Z.-L. Huang, *J. Mol. Struct*., 2007, **833**, 82-87.
59. X. Yin, Y. Li, Y. Zhu, X. Jing, Y. Li, D. Zhu, *Dalton Trans*., 2010, **39**, 9929-9935.
60. Y. Hirata, T. Okada, T. Nomoto, *Chem. Phys. Lett*., 1993, **209**, 397-402.
61. Y. Hirata, T. Okada, T. Nomoto, *Acta Phys. Polon*., 1998, **94**, 627-636.
62. Y. Hirata, T. Okada, T. Nomoto, *J. Phys. Chem*., 1993, **97**, 6677-6681.
63. W. Wiczk, K. Stachowiak, P. Skurski, L. Łankiewicz, A. Michniewicz, A. Rój, *J. Am. Chem. Soc*., 1996, **118**, 8300-8307.
64. T. Fujiwara, M. Z. Zgierski, E. C. Lim, *J. Phys. Chem. A*, 2008, **112**, 4736-4741.

